C-S bond cleavage influenced by metal coordination in Zn(II) bound Schiff base complex: synthesis, structural characterization, catecholase and phenoxazinone synthase activities

Ayon Kanti Ghosh[a], Arnab Chatterjee[a], Sarat Chandra Kumar[a], Chandra Shekhar Purohit[b] & Rajarshi Ghosh [a],*

[a]Department of Chemistry, The University of Burdwan, Burdwan 713 104, India

[b]Department of Chemical Sciences, National Institute of Science Education and Research, Bhubaneswar 751 005, India

Email: rghosh@chem.buruniv.ac.in

A new zinc(II) Schiff base complex (**1**) has been synthesized and X-ray crystallographically characterized. It crystalizes in *P2/c* space group with monoclinic crystal system. One C-S bond in a (N,S,O) donor organic ligand has been found to be cleaved on reaction with the zinc(II) perchlorate hexahydrate to yield **1** with new ligand formulation. Complex **1** is found to be both catecholase and phenoxazinone synthase active in MeOH at room temperature. Michaelis-Menten kinetics for each of the activities has been investigated. The turn over numbers for catecholase and phenoxazinone synthase activities are 4.31×10^2 and 5.27×10^5 h^{-1}, respectively.

Molecular models of the active sites of different metalloenzymes and their use to activate molecular/aerial oxygen for different organic transformations are very much important as the method is easy, green as well as economic[1,2]. Mimicking catechol oxidase is a trend in synthetic coordination chemistry since its discovery in 1998[3-6]. Catechol oxidase is a copper containing protein[7] which catalyses the catechol-quinone conversion (Scheme 1) in the plant tissues. Copper compounds of different nuclearity which catalyse to convert catechol to quinone in laboratory are reported in literature[4-6]. Phenoxazinone synthase is another multicopper oxidase which is found in the bacterium *Streptomyces antibioticus*. This is responsible for six electron oxidative coupling of two molecules of an *o*-aminophenol derivative, 4-methyl-3-hydroxyanthraniloyl pentapeptide to phenoxazinone chromophore (Scheme 2). Few copper complexes which mimic the phenoxazinone synthase are reported in literature[8]. Now a days a number of non-copper complexes of different nuclearity are found in literature which are catalysing catecholase and/or phenoxazinone synthase activities[9-14]. Few redon inactive Zn(II) complexes which are redox inactive are known to catalyse those activities[11,12].

Different synthetic strategies towards synthesis of coordination molecules of different functionalities includes activation (cleavage) of different bonds like C-H[15], C-C [16], C-S[17], etc., upon transition metal coordination. Among these the C-S bond cleavage is important not only in organic synthesis[17] but also in petroleum industry where removal of organo-sulphur compounds present in petroleum-based feedstock[18] is important.
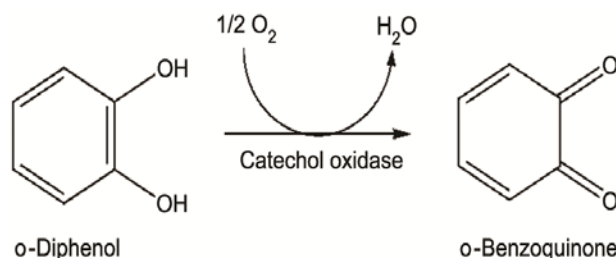
Catecholase activity
Scheme 1
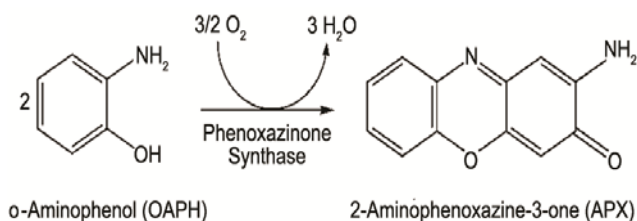
Phenoxazinone synthase activity
Scheme 2

In our present report, synthesis of a mononuclear Zn(II) complex [Zn(L)$_2$] [HL = 2-((E)-(3-mercaptopropylimino)methyl)phenol] (**1**) is found to pass through a C-S bond cleavage in the original organic ligand framework. The synthesized compound is crystallographically characterized and shows catecholase and phenoxazinone synthase activities in MeOH at room temperature.

Materials and Methods

High purity 2-mercaptoethanol, 3-chloropropylamine, salicylaldehyde and zinc(II) perchlorate hexahydrate were purchased from Sigma Adrich, India and used as received.

Elemental analyses (carbon, hydrogen and nitrogen) were performed on a Perkin-Elmer 2400 CHNS/O elemental analyser. IR spectrum was recorded (KBr discs, 4000–300 cm^{-1}) using a Perkin-Elmer RX1 FTIR spectrometer. Ground state absorption was measured with a JASCO V-530 UV-vis spectrophotometer.

Synthesis of H$_2$L′

2-Mercaptoethanol (8 mmol, 0.625 g) was added gradually into the cooled sodium ethoxide solution which was prepared by the addition of metallic sodium to dry ethanol with continuous stirring. Then 3-chloropropylamine (8 mmol, 1.04 g) was added slowly to this reaction mixture and the mixture was stirred for about 1 h. During this stirring, sodium chloride was precipitated , which confirms the formation of the 2-(3-aminopropylthio)ethanol (Scheme 3).The precipitated sodium chloride was

separated by filtration. Salicyaldehyde (8 mmol, 0.97 g) was added to this solution of 2-(3-aminopropylthio)ethanol and this mixture was refluxed for 4 h. The ligand H$_2$L′ was thus obtained. The synthesized H$_2$L′ was extracted from the mixture by solvent extraction.

Yield, 1.434 g (75% based on aldehyde). Anal (%):Calc.: C$_{12}$H$_{17}$NO$_2$S (HL): C, 60.22; H, 7.16; N, 5.85. Found: C, 60.12; H, 7.23; N, 5.89. IR cm^{-1} (KBr): 3361s, 2866-2922w. 1629(s), 754(m); UV-vis (MeOH, nm): λ_{max} nm: 214, 254, 315, 401. ^{1}H NMR δ (ppm): 2.17 (q, J = 6.4 Hz, 2H), 2.63 (t, J = 7.2 Hz, 2H), 2.88 (t, J = 6.0 Hz, 2H), 3.62 (t, J = 6.0 Hz, 2H), 3.90 (t, J = 6.0 Hz, 2H), 6.87–6.89 (m, 1H), 6.90–6.96 (m, 1H), 7.23–7.27 (m, 1H), 7.28–7.33 (m, 1H), 8.37 (d, J = 10.8 Hz, 1H), 13.28 (bs, 1H).

Synthesis of Complex 1

Solid zinc(II) perchlorate hexahydrate (0.1 mmol, 0.037 g) was slowly added to the hot ethanolic solution of H$_2$L′ (0.2 mmol, 0.048 g) with continuous stirring for 3 h. The brown colour of the ligand solution changed to pale yellow on dissolution of the metal salt. This reaction mixture was kept open in air for slow evaporation. Light orange coloured X-ray quality crystals of **1,** where one C-S bond of the ligand framework was found to be cleaved were obtained after keeping the solution in open air after a week or so. This resulted in a new Zn(II) bound ligand HL (molecular structure of the complex was confirmed X-ray crystallographically later) (Scheme 3).

Yield, 0.03174g (70% based on metal salt). Anal (%):Calc.: C$_{20}$H$_{24}$N$_2$O$_2$S$_2$Zn (**1**): C, 52.87; H, 5.32;
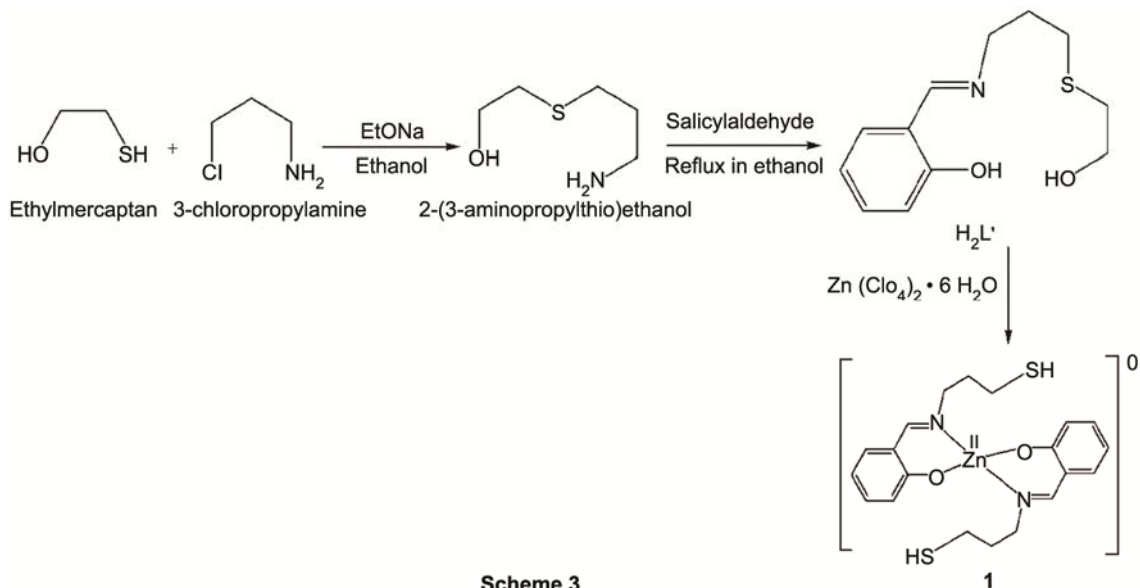
Scheme 3

N, 6.17. Found: C, 52.51; H, 5.35; N, 6.14. IR cm^{-1}(KBr): 2915s, 1622s, 752s, 654s. UV-vis (MeOH, nm): λ_{max} (ϵ) at 239, 258, 321 and 363.

X-ray diffraction study

A summary of the crystallographic data and structure refinement parameters are given in Table 1. Single crystals [size: 0.23×0.30×0.38 mm^3] of **1** were obtained by slow evaporation of MeOH-H$_2$O solution of the reaction mixture. Light orange crystals suitable for X-ray crystallographic analysis were selected following examination under a

Table 1 — Crystal data and structure refinement parameter of compound 1

CCDC No.	1563187
Emperical formula	C$_{20}$H$_{24}$N$_2$O$_2$ S$_2$Zn
Formula weight	453.96
Temperature (K)	293(2)
Wavelenght (Å)	0.71073
Crystal system	Monoclinic
Space group	*P2/c*
Unit cell dimensions	
a (Å)	18.4340(7)
b (Å)	5.7108(2)
c (Å)	20.3467(7)
α (°)	90
β (°)	97.354(2)
γ (°)	90
Volume (Å^3)	2124.34(13)
Z	4
Calculated densisty D$_{calc}$ (mg m^{-3})	1.820
Absorption coefficient(mm^{-1})	1.600
F(000)	1176
Crystal size (mm^3)	0.38×0.3×0.23
Theta range for data collection (°)	1.114 - 25.378
Index ranges	$-22 \leq h \leq 22$, $\;-5 \leq k \leq 6$, $-24 \leq l \leq 24$
Reflections collected	19576
Independent reflections	3886 [R$_{int}$ = 0.0475]
Completeness of theta	99.8 % [θ = 25.378]
Absorption correction	Multi-scan
T$_{max}$ and *T$_{min}$*	0.5969 and 0.7452
Refinement method	Full matrix
Data/restrains/parameters	3886/0/ 236
Goodness-of fit (GOF) *F^2*	1.041
Final *R* index [*l* >2σ(*l*)]	*R$_1$* = 0.0559 and w*R$_2$* = 0.1526
R index (all data)	*R$_1$* = 0.0946 and w*R$_2$* = 0.1790
Largest difference between peak and hole (e Å^{-3})	0.607, −0.439

microscope. Diffraction data at 293(2) K were collected on a Smart Apex CCD diffractometer using Mo-K$_\alpha$ radiation (λ = 0.71073 Å). Systematic absence led to the identification of space group *P2/c*. The structure was solved by direct methods, and the structure solution and refinement were based on $|F|^2$. All non-hydrogen atoms were refined with anisotropic displacement parameters whereas hydrogen atoms were placed in calculated positions where possible and given isotropic *U* values 1.2 times that of the atom to which they are bonded. At convergence the final residuals were *R1* = 0.0559; *wR2* = 0.1526 with I>2σ(I), goodness-of-fit = 1.041. The final differences Fourier map showed the maximum and minimum peak heights at 0.573 and -0.493 e Å^{-3}. All calculations were carried out using SHELXTL 5.10[19].

Results and Discussion

Synthesis and formulation

The organic ligand H$_2$L′ was prepared by abstracting the proton of 2-mercaptoethanol by sodium ethoxide which was prepared *in situ*. 3-Chloropropylamine was mixed with this reaction mixture to get 2-(3-aminopropylthio)ethanol which on further condensation with salicyaldehyde resulted in the ligand H$_2$L′. This was characterized through proton NMR (Supplementary Data, Fig. S1a and S1b). Zinc(II) perchlorate was added to the solution of the H$_2$L′ with stirring. This produced the metal complex **1** which on single crystal X-ray diffraction revealed that one of the C-S bonds in the ligand framework was cleaved and the zinc(II) complex of HL (which appeared as a new metal bound ligand) was generated. C-S bond cleavage in presence of metal salts reported in literature[17]. As we used Zn(II) perchlorate for the synthesis of the metal complex, a question may arise whether the resulting perchloric acid resulted in the reaction is cleaving the C-S bond of the ligand framework or not. To evaluate this aspect we repeated the reaction with Zn(II) acetate and got the same complex with the same molecular structure as from the single crystal X-ray diffraction (Supplementary Data, Table S1). Here the resulting acetic acid being weak might not be able to cleave the C-S bond. So it is clearly seen that metal coordination is playing the sole role for this very cleavage and not the acid which was formed as a by-product.

X-ray structure

The thermal plot (ORTEP) of **1** and X-ray crystallographic data are provided in Fig. 1 and Table 1, respectively. Complex **1** crystalizes in *P2/c* space group. Considering bond angle and bond distance data (Table 2) coordination geometry around zinc(II) centre is best described as distorted tetrahedron. Only the imine nitrogens [N(2) and N(2^i)] and phenoxy oxygens [O(1) and O(1^i)] are coordinated to *meta* centres. The thiol groups remain uncoordinated. The maximum and minimum bond distances of the metal centre with the coordinated atoms are 2.005 and 1.917 Å (Δ = 0.088 Å) respectively.

Catecholase activity

Spectrophotometric study

The catecholase activity study was carried out using the substrate 3,5-di-*tert*-butyl catechol (3,5-DTBC) having two bulky *t*-butyl substituents on the ring and low quinone-catechol reduction potential.
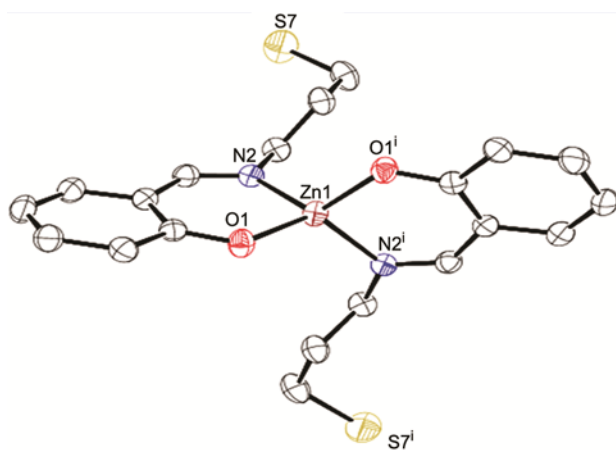

Fig. 1 — ORTEP of Complex **1** with 20% ellipsoid probability (hydrogen atoms have been excluded for clarity).

Table 2 — Bond lengths (Å) and bond angles (°) of compound 1

Bond lengths (Å)	
Zn(1)-O(1)	1.917(3)
Zn(1)-O(1′)	1.917(3)
Zn(1)-N(2)	2.005(4)
Zn(1)-N(2′)	2.005(4)
Bond angles (°)	
O(1)-Zn(1)-N(2)	95.85(14)
O(1)-Zn(1)-N(2′)	122.77(15)
O(1)-Zn(1)- O(1′)	108.7(2)
O(1′)-Zn(1)-N(2)	95.85(14)
O(1′)-Zn(1)-N(2′)	122.77(15)
N(2)-Zn(1)-N(2′)	113.0(2)

This makes it easily oxidizable to the corresponding o*rtho*-quinone derivative 3,5-di-*tert*-butyl quinone (3,5-DTBQ) which is highly stable and shows a maximum absorption at 401 nm in methanol[20]. Spectral bands at 239, 258, 321 and 363 nm appear in the electronic spectrum of complex **1**, whereas 3,5-DTBC shows a single band at 282 nm. Upon treatment of methanolic solution of 1 equivalent of **1** into 100 equivalents of 3,5-DTBC under aerobic conditions, the repetitive UV-vis spectral scan was recorded (Fig. 2). The colourless solution gradually turned deep brown which indicated conversion of 3,5-DTBC to 3,5-DTBQ. In UV-vis spectrophotometer, after this addition, the spectral scan shows very smooth increase of a quinone band at around ~390 nm which shifts ultimately to 401 nm, as reported by Krebs *et al*[20]. The same reaction was carried out by scaling up the reagents and 3,5-DTBQ was purified by column chromatography. Chromatographically pure 3,5-DTBQ was characterized by determining its melting point (~110 °C) which agreed well with that reported in literature[21].

The time dependent change in absorbance at a wavelength of 401 nm, which was characteristic of 3,5-DTBQ in methanol, was observed for 60 min to comprehend the reaction kinetics and find out the reaction rate between 3,5-DTBC and **1**. The difference in absorbance Δ*A* at 401 nm, was plotted against time to obtain the rate/velocity for that particular catalyst to substrate concentration ratio (Supplementary Data, Fig. S2). A first-order catalytic reaction is observed, with rate $3.36×10^{-4}$ min^{-1}.

Control experiments were done with only 3,5-DTBC, and 3,5-DTBC and Zn(II) perchlorate in methanol. No peak growth at ~400 nm was observed
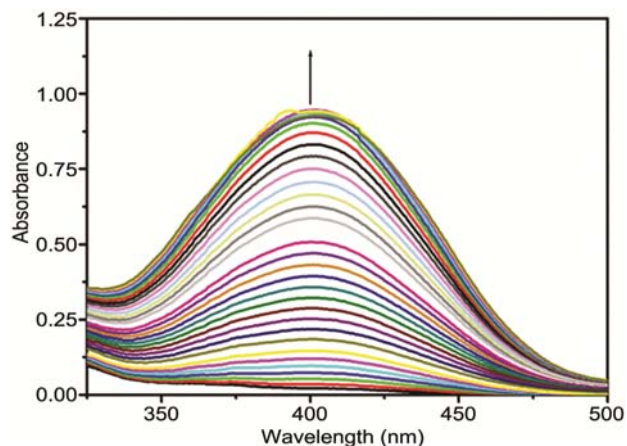

Fig. 2 — Change in spectral pattern of complex **1** after reaction with 3,5-DTBC (the reaction was observed for 6 h in methanol).

in UV-vis repetitive scan which continued for 2 h (Supplementary Data, Figs. S3 and S4).

Enzyme kinetics study

Kinetic experiments were performed spectrophotometrically with complex **1** and the substrate 3,5-DTBC in methanol, thermostated at 20 °C. The complex solution (0.04 mL), with a constant concentration of 1×10^{-4} M, was added to 2 mL of 3,5-DTBC of a particular concentration (varying its concentration from 1×10^{-3} M to 1×10^{-2} M) to achieve the final concentration of the complex as 1×10^{-4} M. The conversion of 3,5-DTBC to 3,5-DTBQ was monitored with time at a wavelength of 401 nm for solutions in MeOH. The rate for each concentration of the substrate was determined by the initial rate method.

The rate versus concentration of substrate data were analyzed on the basis of Michaelis-Menten approach of enzymatic kinetics to obtain the Lineweaver-Burk (double reciprocal) plot as well as the values of the various kinetic parameters viz., V_{max}, K_M and K_{cat}. The observed rate versus [substrate] plot as well as Lineweaver-Burk plot in methanol solutions are given in Fig. 3. The kinetic parameters are listed in Supplementary Data, Table S2. The turnover number (K_{cat}) is 4.31×10^2 h^{-1}.

Reaction mechanism

The catalytic process follows a two-step mechanistic pathway. The first step is the rate determining step. Probably, in this step, the 1:1 adduct of catechol and the zinc complex is formed and a 1:100 mixture of complex **1** and 3,5-DTBC is obtained. The complex **1** exhibits a peak at m/z = 453.64 (Supplementary Data, Fig. S5). The peak at m/z = 243.56 can be assigned to sodium aggregate of
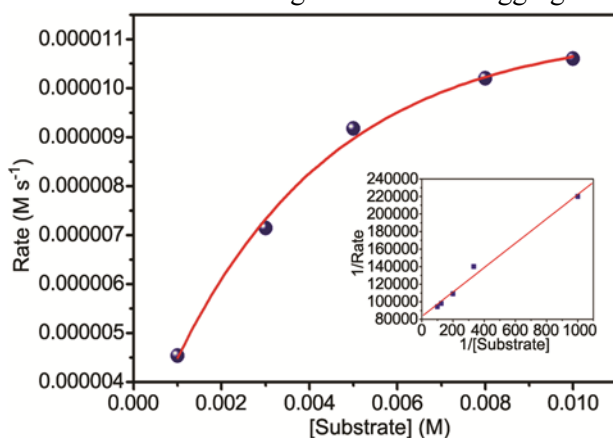
quinone [3,5-DTBQ]-Na$^+$ (Supplementary Data, Fig. S6). To obtain a mechanistic inference of the catecholase activity and to get an idea about the complex-substrate intermediate, the formation of a complex-substrate adduct is identified by the peak at m/z = 675.59 (Supplementary Data, Fig. S7). The proposed structure of this adduct is given in Scheme 4. The catechol derivative, 3,5-DTBC gets oxidised to quinone in presence of oxygen. The aerial oxygen that oxidises 3,5-DTBC to 3,5-DTBQ in this process is converted to H$_2$O$_2$. H$_2$O$_2$ thus liberated was identified and characterized spectrophotometrically. Details of spectrophotometric detection of H$_2$O$_2$ in the oxidation reaction[22] are given as supplementary data.

Phenoxazinone synthase activity
Spectrophotometric study

The phenoxazinone synthase activity study was carried out using the substrate *o*-aminophenol (OAPH). OAPH shows bands at 286 and 232 nm in

Catechol-complex adduct
Scheme 4

Fig. 3 — Plot of rate versus [substrate] (3,5-DTBC) in presence of **1** in MeOH. [Inset: Lineweaver-Burk plot].
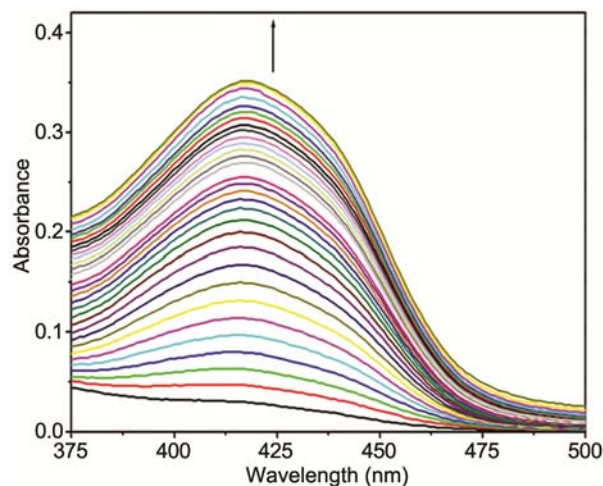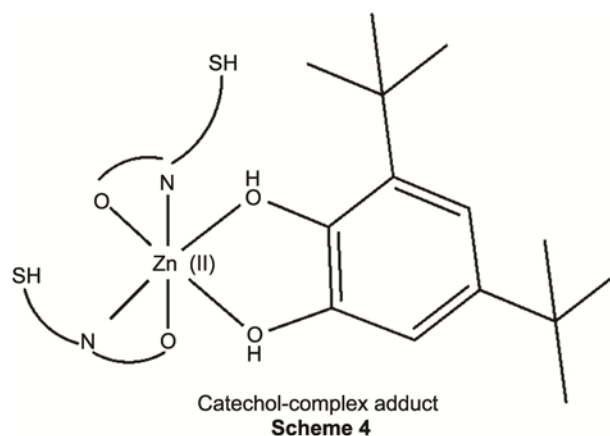
Fig. 4 — Change in spectral pattern of complex **1** after reaction with OAPH (the reaction was observed for 6 h in methanol).
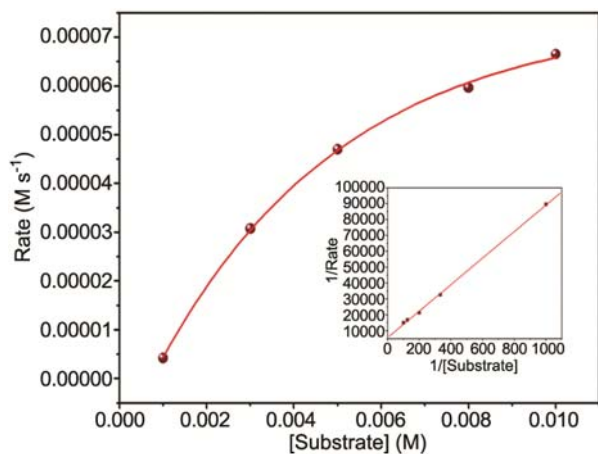
Fig. 5 — Plot of rate versus [substrate] (OAPH) in presence of **1** in MeOH. [Inset: Lineweaver-Burk plot].

pure methanol. Upon treatment of methanolic solution of **1** into 100 equivalents of OAPH under aerobic conditions, the repetitive UV-vis spectral scan was recorded (Fig. 4). The colourless solution gradually turned deep brown which indicates conversion of OAPH to 2-aminophenoxazine-3-one (APX). The spectral scan shows very smooth growth of APX band at 427 nm[8c]. APX was identified by HRMS with m/z = 235.54 (sodium aggregate of APX) (Supplementary Data, Fig. S8). The time dependent change in absorbance at a wavelength of 427 nm, characteristic of APX in methanol, was observed for 50 min to comprehend the reaction kinetics and find out the reaction rate between OAPH and **1**. The difference in absorbance ΔA at 427 nm, was plotted against time to obtain the initial rate for that particular catalyst to substrate concentration ratio (Supplementary Data, Fig.S9). A first-order catalytic reaction is observed, with initial rate 1.64×10^{-2} min^{-1}.

Control experiments were carried out with only OAPH, and, OAPH and Zn(II) perchlorate in methanol. In reaction with only OAPH, a UV-vis peak growth suggesting the formation of phenoxazinone was found (Supplementary Data, Fig. S10), but the peaks were not very regular as with **1** (Fig. 4). No band for phenoxazinone (in the UV-vis repetitive scan) was found in the reaction mixture of OAPH and Zn(II) perchlorate (Supplementary Data, Fig. S11).

Enzyme kinetics study

Enzymatic kinetic experiments were performed using UV-vis spectrophotometry under thermostated condition at 25 °C with complex **1** and the substrate OAPH in MeOH. The complex solution (0.04 mL),

with a constant concentration of 1×10^{-4} M, was added to 2 mL of OAPH of a particular concentration (varying its concentration from 1×10^{-3} M to 1×10^{-2} M) to achieve the final concentration of the complex as 1×10^{-4} M. The conversion of OAPH to APX was monitored with time at a wavelength of 417 nm for solutions in MeOH. The rate for each concentration of the substrate was determined by the initial rate method. The rate versus concentration of substrate data, were analyzed on the basis of Michaelis-Menten approach of enzymatic kinetics to get the Lineweaver-Burk (double reciprocal) plot as well as the values of the various kinetic parameters viz., V_{max}, K_M and K_{cat}. The observed rate versus [substrate] plot in methanol solution as well as Lineweaver-Burk plot is given in Fig. 5. The kinetic parameters are listed in Supplementary Data, Table S3. The turnover number (K_{cat}) is 5.27×10^5 h^{-1} in methanol.

Reaction mechanism

To elucidate mechanistic pathway of the reaction, it is found that initially OAPH forms an adduct with **1** which is trapped by mass spectrometry at m/z = 564.46 (OAPH-**1**) (Supplementary Data, Fig. S12). This adduct generates 2-amoinophenoxazine-3-one through some intermediate reaction with molecular oxygen. Reduced molecular oxygen in the form of H_2O_2 was detected spectrophotometrically (details are provided as supplementary data)[22].

Conclusions

Synthesis and X-ray crystallographic structure of Complex **1** along with C-S bond cleavage of its organic ligand backbone during its synthesis has been reported. The compound is found to catalyse both catechol to quinine, and 2-aminophenol to corresponding phenoxazinone chromophore reactions. Some other Zn(II) complexes of different nuclearities have been reported in literature, which catalyze 3,5-DTBC[11,12]. To the best of our knowledge no Zn(II) complexes were found to show phenoxazinone synthase activity so far. The turn over number for the catecholase activity is found to be better than a reported work[13b]. Similarly, the turn over number for compound (**1**) of phenoxazinone synthase activity is also better than one the reported in literature[14].

Supplementary Data

Crystallographic data for the structural analysis of complex 1 have been deposited with Cambridge Crystallographic Data Centre, under CCDC No. 1563187. Copy of this information may be obtained

free of charge from: The Director, CCDC, 12 Union Road, Cambridge CB2 1EZ, UK (fax: 44-1223-336-033: Email: deposit@ccdc.cam.ac.uk). Other supplementary data associated with this article are available in the electronic form at http://www.niscair.res.in/jinfo/ijca/IJCA_57A(11) 1351-1357_SupplData.pdf.

Acknowledgement

References

1. (a) Costas M, Mehn M P, Jensen M P & Que Jr L, *Chem Rev*, 104 (2004) 939; (b) Company A, Prat I, Frisch J R, Mas-Ballest R, Güell M, Juh ász G, Ribas X, Münck E, Luis J M, Que Jr L & Costas M, *Chem Eur J*, 17 (2011) 1622; (c) Prat I, Company A, Postils V, Ribas X, Que Jr L, Luis Jr J M & Costas M, *Chem Eur J*, 19 (2013) 6724; (d) McDonald A R, Heuvelen K M V, Guo Y, Li F, Bominaar E L, Münck E & Que Jr L, *Angew Chem Int Ed*, 51 (2012) 9132.

2. (a) Paria S, Que Jr L and Paine T K, *Angew Chem Int Ed*, 50 (2011) 11129; (b) Chakraborty B, Halder P, Banerjee P R & Paine T K, *Eur J Inorg Chem*, (2012) 5843; (c) Mukherjee A, Cranswick M A, Chakrabarti M, Paine T K, Fujisawa K, Münck E & Que Jr L, *Inorg Chem*, 49 (2010) 3618; (d) Dutta S, Peng S M & Bhattacharya S, *Inorg Chem*, 39 (2000) 2231.

3. Klabunde T, Eicken C, Sacchettini J C & Krebs B, *Nat Struct Biol*, 5 (1998) 1084.

4. (a) Abuhijleh A L, Pollitte J & Woods C, *Inorg Chim Acta*, 215 (1994) 131; (b) Malachowski M R, Davidson M G & Hoffman J N, *Inorg Chim Acta*, 157 (1989) 91; (c) Malachowski M R & Davidson M G, *Inorg Chim Acta*, 162 (1989) 199; (d) Mitra M, Maji A K, Ghosh B K, Kaur G, Choudhury A R, Lin C H, Ribas J & Ghosh R, *Polyhedron*, 61 (2013) 15.

5. (a) Koval I A, Selmeczi K, Belle C, Philouze C, Saint-Aman E, Gautier-Luneau I, Schuitema A M, van Vliet M, Gamez P, Roubeau O, Lüken M, Krebs B, Lutz M, Spek A L, Pierre J L & Reedijk J, *Chem Eur J*, 12 (2006) 6138; (b) Merkel M, Mçller N, Piacenza M, Grimme S, Rompel A & Krebs B, *Chem Eur J*, 11 (2005) 1201; (c) Thio Y, Yang X & Vittal J J, *Dalton Trans*, 43 (2014) 3545; (d) Banu K S, Chattopadhyay T, Banerjee A, Bhattacharya S, Suresh E, Nethaji M, Zangrando E & Das D, *Inorg Chem*, 47 (2008) 7083; (e) Dasgupta S, Majumder I, Chakroborty P, Zangrando E, Bauza A, Frontera A & Das D, *Eur J Inorg Chem*, (2017) 133.

6. (a) Majumder S, Sarkar S, Sasmal S, Sanudo E C & Mohanta S, *Inorg Chem*, 50 (2011) 7540; (b) Mijangos E, Reedijk J &

Gasque L, *Dalton Trans*, 2008, 1857; (c) M Mitra M, Kundu T, Kaur G, Sharma G, Choudhury A R, Singh Y & Ghosh R, *RSC Adv*, 6 (2016) 58831.

7. (a) Koval I A, Gamez P, Belle C, Selmeczi K & Reedijk J, *Chem Soc Rev*, 35 (2006) 814; (b) Dey S K & Mukherjee A, *Coord Chem Rev*, 310 (2016) 80.

8. (a) Maurya M R, Sikarwar S, Joseph T & Halligudi S B, *J Mol Cat A: Chemical*, 236 (2005) 132; (b) Mukherjee C, Weyhermüller T, Bothe E, Rentschler E & Chaudhuri P, *Inorg Chem*, 46 (2007) 9895.

9. (a) Kar P, Ida Y, Kanetomo T, Drew M G B, Ishida T & Ghosh A, *Dalton Trans*, 44 (2015) 9795; (b) Chakraborty P, Majumder S, Jana A & Mohanta S, *Inorg Chim Acta*, 410 (2014) 65; (c) Das M, Nasani R, Saha M, Mobin S M & Mukhopadhyay S, *Dalton Trans*, 44 (2015) 2299.

10. (a) Singh R, Banerjee A & Rajak K K, *Inorg Chim Acta*, 363 (2010) 3131; (b) Mitra M, Maji A K, Ghosh B K, Raghavaiah P, Ribas J & Ghosh R, *Polyhedron*, 67 (2014) 19; (c) Mahapatra T S, Basak D, Chand S, Lengyel J, Shatruk M, Bertolasi V & Ray D, *Dalton Trans*, 45 (2016) 13576; (d) Mitra M, Raghavaiah P & Ghosh R, *New J Chem*, 39 (2015) 200.

11. (a) Guha A, Chattopadhyay T, Paul N D, Mukherjee M, Goswami S, Mondal T K, Zangrando E & Das D, *Inorg Chem*, 51 (2012) 8750; (b) Mal S K, Mitra M, Purohit C S & Ghosh R, *Polyhedron*, 101 (2015) 191; (c) Sanyal R, Dash S K, Das S, Chottopadhyay S, Roy S & Das D, *J Biol Inorg Chem*, 19 (2014) 1099; (d) Kaizer J, Pap J, Speier G, Parkanyi L, Korecz L & Rockenbauer A, *J Inorg Biochem*, 91 (2002) 190; (e) Nanjundan N, Narayanasamy R, Geib S, Velmurugan K, Nandhakumar R, Balakumaran M D & Kalaichelvan P T, *Polyhedron*, 110 (2016) 203.

12. Dhara A K, Singh U P & Ghosh K, *Inorg Chem Front*, 3 (2016) 1543.

13. (a) Baruah B & Chakravorty A, *Indian J Chem*, 42A (2003) 2677; (b) Mal S K, Mitra M, Yadav H R, Purohit C S, Choudhury A R & Ghosh R, *Polyhedron*, 111 (2016) 118.

14. (a) Mitra M & Ghosh R, *Indian J Chem*, 55A (2016) 681; (b) Panja A, *RSC Adv*, 4 (2014) 37085; (c) Panja A, *Dalton Trans*, 43 (2014) 7760; (d) Panja A, Shyamal M, Saha A & Mandal T K, *Dalton Trans*, 43 (2014) 5443; (e) Kumar S C, Ghosh A K, Chen J D & Ghosh R, *Inorg Chim Acta*, 464 (2017) 49.

15. (a) Lyons T W & Sanford M S, *Chem Rev*, 110 (2010) 1147; (b) Acharyya R, Basuli F, Wang R -Z, Mak T C W & Bhattacharyya S, *Inorg Chem*, 43 (2004) 704.

16. (a) Chakraborty B, Halder P, Banerjee P R & Paine T K, *Eur J Inorg Chem*, (2012) 5843; (b) Paria S, Halder P & Paine T K, *Angew Chem Int Ed*, 51 (2012) 6195

17. (a) Jana M & Majumdar A, *Inorg Chem*, 57 (2018) 617; (b) Das B, Sarkar S, Zangrando E & Chattopadhyay P, *Inorg Chem Comm*, 12 (2009) 1112

18. (a) Bianchini C, Meli A, *Acc Chem Res* 31 (1998) 109; (b) Choudhary T V, Malandra J, Green J, Parrott S, Johnson B, *Angew Chem Int Ed*, 45 (2006) 3299.

19. Sheldrick G M, *Acta Crystallogr, Sect A: Found Crystallogr*, 64 (2008) 112.

20. Zippel F, Ahlers F, Werner R, Haase W, Nolting H F & Krebs B, *Inorg Chem*, 35 (1996) 3409.

21. Tsuruya S, Yanai S I & Masai M, *Inorg Chem*, 25 (1986) 141.

22. Vogel A I, *Textbook of Quantitative Inorganic Analysis, 3rd edn*, (Longmans, Green and Co. Ltd, London), 1961 p. 366.